Exploring spin valve magnetization reversal dynamics with temporal, spatial and layer resolution: Influence of domain-wall energy

W. Kuch[a)]
Max-Planck-Institut für Mikrostrukturphysik, Weinberg 2, D-06120 Halle, Germany

J. Vogel
Laboratoire Louis Néel, CNRS, 25 avenue des Martyrs, B.P. 166, F-38042 Grenoble Cedex 9, France

J. Camarero
Departamento de Física de la Materia Condensada, Universidad Autónoma de Madrid, E-28049 Madrid, Spain

K. Fukumoto
Max-Planck-Institut für Mikrostrukturphysik, Weinberg 2, D-06120 Halle, Germany

Y. Pennec, S. Pizzini, and M. Bonfim[b)]
Laboratoire Louis Néel, CNRS, 25 avenue des Martyrs, B.P. 166, F-38042 Grenoble Cedex 9, France

J. Kirschner
Max-Planck-Institut für Mikrostrukturphysik, Weinberg 2, D-06120 Halle, Germany

(Received 15 March 2004; accepted 21 May 2004)

The magnetization reversal dynamics of an $Fe_{20}Ni_{80}/Cu/Co$ spin valve is investigated on the nanosecond time scale by magnetic microscopy with time and layer resolution. It is found that the speed by which micron-sized magnetic domains in the magnetically soft $Fe_{20}Ni_{80}$ layer are expanded by external field pulses exhibits a dependence on the change in domain-wall length, and on the coupling to the local magnetization direction of the Co layer. © *2004 American Institute of Physics*. [DOI: 10.1063/1.1772520]

Controlling and understanding the magnetization reversal dynamics in magnetic thin films is a major issue for many applications. An example for magnetic thin-film devices is giant magnetoresistance spin valves, as they are nowadays commonly used in magnetic hard disk read heads. Spin valves are also expected to play a major role in future applications like magnetic random access memories, or in integrating magnetism into electronic devices.[1] A spin valve consists in the simplest case of two ferromagnetic layers coupled through an ultrathin nonmagnetic spacer layer. Operation relies on the independent manipulation of the magnetization state of one of the magnetic layers, which has to be performed with high speed in order to meet the increasing demands for high data rates. Fast dynamic measurements of the magnetic reversal behavior in such coupled systems are therefore highly desired.

Only very few experimental techniques can address the microscopic magnetization reversal behavior of the different magnetic layers in a spin valve separately. One of them is photoelectron emission microscopy (PEEM) with x-ray magnetic circular dichroism (XMCD),[2] which has already proven its versatility for the layer-resolved investigation of microscopic magnetic domains in multilayered magnetic samples.[3,4] It has been demonstrated recently that XMCD-PEEM can also be used in a time-resolved pump–probe measurement scheme to address the dynamic response of a system on short magnetic field pulses,[5,6] however, the layer resolution has not been exploited in these studies. In dynamic XMCD-PEEM measurements, the pulsed nature of synchrotron radiation *x* rays is used to probe the sample magnetization in a stroboscopic way at a certain tunable delay after periodic application of short magnetic field pulses. By tuning the photon energy to elemental absorption edges, the magnetic domain patterns in magnetic layers containing different elements can be imaged separately.

In this letter, we combine the temporal, spatial, and layer resolution of time-resolved XMCD-PEEM to study the magnetization reversal dynamics of a $Fe_{20}Ni_{80}/Cu/Co$ spin valve on the nanosecond time scale. We find that, due to the variation of the overall domain-wall length, the dynamic magnetization reversal of the magnetically softer $Fe_{20}Ni_{80}$ layer is determined by the domain-wall energy in the $Fe_{20}Ni_{80}$ layer, and by the local magnetic interlayer coupling to the domain structure of the Co layer.

The magnetization reversal in laterally extended magnetic thin films proceeds by nucleation and expansion of magnetic domains. Since these processes are usually thermally activated, the speed of magnetization reversal depends exponentially on the effective field H_{eff} which promotes domain-wall propagation across statistically distributed energy barriers. Small changes of the energy gain upon domain-wall propagation $E_{\mathrm{prop}}=-H_{\mathrm{eff}}M_S t$ may thus have a big effect on the speed of reversal. Here, M_S denotes the saturation magnetization, and t is the layer thickness. We will show that for a proper description of E_{prop} and of the reversal speed not only the applied external field H_{ext} has to be considered, but also contributions from the magnetic interlayer coupling energy $E_{\mathrm{copl}}=-J\cos\Delta\phi$, where $\Delta\phi$ denotes the local angle between the magnetization directions in the two ferromagnetic layers, and from the change in domain-wall energy ΔE_{DW}. The latter reflects the change of domain-wall length during the reversal.

[a)]Electronic mail: kuch@mpi-halle.de
[b)]Present address: Departamento de Engenharia Elètrica, Universidade do Paraná, CEP 81531-990, Curituba, Brazil.

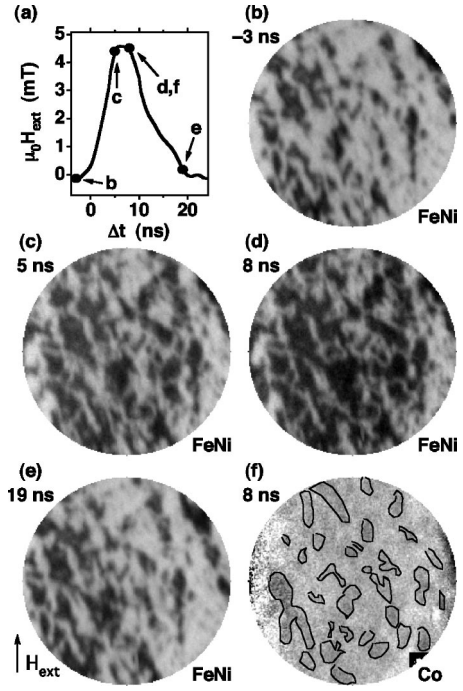

FIG. 1. Time- and layer-resolved magnetic domain images of a 5 nm $Fe_{20}Ni_{80}$/4 nm Cu/5 nm Co spin valve. (a) Temporal shape of the magnetic field pulses, and times at which domain images presented in (b)–(f) were acquired. (b)–(e) Layer-resolved stroboscopic magnetic domain images of the $Fe_{20}Ni_{80}$ layer at delays Δt of −3, 5, 8, and 19 ns, respectively, between beginning of the field pulse and probe pulse. (f) Layer-resolved stroboscopic magnetic domain image of the Co layer at 8 ns delay. Field of view: 25 μm.

The spin valve sample studied here consisted of 5 nm $Fe_{20}Ni_{80}$/4 nm Cu/5 nm Co, deposited on a SiO_2/Si(001) substrate by rf sputtering. Quasistatic Kerr effect measurements showed no magnetic anisotropy within the film plane, and a weak magnetic interlayer coupling with a distribution of coupling energies around $J=1.6\times10^{-6}$ J/m^2.[7] Stroboscopic time-resolved domain images were acquired using an electrostatic PEEM (Focus IS-PEEM), which has been described in a previous publication.[8] Parameters were set to result in a lateral resolution of 300 nm, and a field of view of 25 μm.

X-ray pulses from the UE52-SGM helical undulator beamline of BESSY in single bunch mode of operation were incident to the sample under an angle of 60° from the surface normal. Magnetic pulses were applied along the projection of the x-ray incidence direction on the sample surface by a microcoil made from 12.5 thick μm Cu foil at 625 kHz frequency, which is one-half of the repetition rate of the synchrotron pulses of 50−70 ps length emitted in the single bunch mode of the BESSY storage ring. Electrons originating from the x-ray pulses that do not correspond to a magnetic field pulse were suppressed by a gated negative voltage supplied to a grid in front of the image intensifier of the microscope. A complete description of the experimental setup and time scheme can be found in Ref. 5.

Magnetic pulses with a maximum field strength of 3.58 kA/m, duration of 18 ns, and 5 ns rise time were used, as displayed in Fig. 1(a). The pulse shape was determined from the displacement of the PEEM image provoked by the Lorentz force acting on electrons leaving the sample surface. The field amplitude was calibrated by Faraday rotation measurements on a paramagnetic sample, as described in Ref. 7.

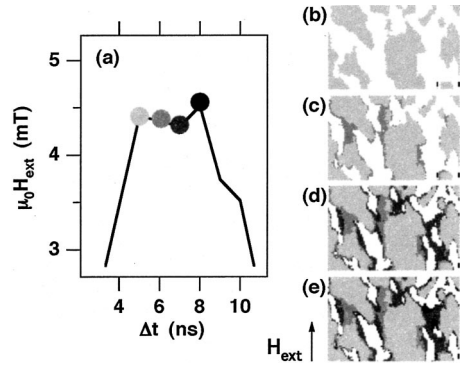

FIG. 2. (a): Magnified view of the maximum of the magnetic field pulses vs time. (b)–(e) Analysis of switching by expansion of domains, extracted from differences between discretized layer-resolved magnetic domain images of the $Fe_{20}Ni_{80}$ layer acquired every 1 ns during the plateau of the field pulse. Differently gray shaded areas correspond to reversed domains present in the $Fe_{20}Ni_{80}$ layer after the time delays indicated in (a) i.e., (b) 5 ns, (c) 6 ns, (d) 7 ns, and (e) 8 ns.

Figures 1(b)–1(f) show layer-resolved magnetic domain images for four different representative delays Δt between field pulse and x-ray pulse, as indicated in panel (a). Panels (b)–(e) display the domain structure of the $Fe_{20}Ni_{80}$ (permalloy) layer and panel (f) shows the domain structure of the Co layer. The images show small and irregularly shaped dark and bright domains, corresponding to magnetization direction parallel and antiparallel to the external field H_{ext} indicated at the left-hand side bottom, respectively. The surface fraction covered by dark domains increases from (b) to (c) to (d) mainly by the expansion of existing dark domains. Interestingly, these domains already shrink when going from (d) to (e), while the external field is still in the "dark" direction. This has to be attributed to the coupling field with the domain structure of the Co layer. This coupling field and a small negative overshoot of the field pulse at $\Delta t \approx 20$ ns help to reversibly bring back the magnetization to the configuration before the field pulse shown in panel (b). Comparison of the contrast between dark and bright domains with images acquired in static conditions revealed that the periodic reversal was fully reproducible over many billions of pulses. No changes for different time delays were observed in the domain pattern of the Co layer, which is displayed in Fig. 1(f) for one time delay Δt [the same as for panel (d)]. The statistics of the Co domain image is worse compared to the permalloy images because of electron attenuation by the relatively thick Cu and $Fe_{20}Ni_{80}$ overlayers. Small black lines in Fig. 1(f) indicate the largest dark domains in the Co layer.

The maximum of the field pulse contains a 3 ns wide plateau where the field is almost constant [Fig. 1(a)]. Here, information on reversal dynamics under a constant field can be separated from the influence of changing external field. Figure 2 shows a detailed analysis of the dynamics of domain expansion during that time. Panel (a) presents a blown up view of the maximum of the field pulse. $Fe_{20}Ni_{80}$ domain images have been acquired at delays of 5, 6, 7, and 8 ns, as marked by symbols of different gray shade. Panels (b)–(e) show how the reversed domains expand as a function of time at that four delays. Bright gray areas correspond to regions in which reversed domains already existed at $\Delta t = 5$ ns. Panel (b) thus represents a discretized version of Fig. 1(c). Areas plotted in different darker shades of gray in subsequent panels correspond to the times indicated by the symbols of cor-

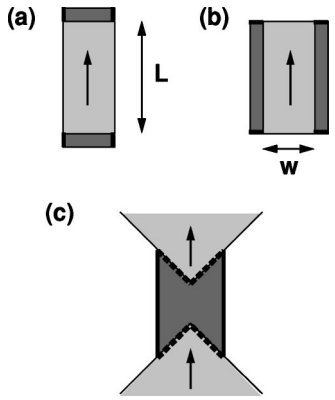

FIG. 3. Schematic explanation for the increase or change in domain-wall length upon magnetization reversal. (a) Expansion of a rectangular domain of length L and width w along the magnetization axis, (b) expansion of the same domain along its width, and (c) merging of two domains. The increase of the domain area by the darker area is accompanied by the creation of domain-wall sections depicted by fat solid lines. While in cases (a) and (b), the total domain-wall length is increasing, in case (c) the domain-wall sections shown by dotted lines disappear, leading to a more favorable domain-wall energy balance and higher domain-wall speeds.

responding shade of gray in Fig. 2(a). The biggest changes, i.e., the largest intermediate and darker gray areas in Fig. 2(e), are seen in regions where two existing domains are getting connected. In these areas, the evolution of reversed domains is somehow reminiscent of merging water droplets. The domain-wall speed can be estimated from Fig. 2, and is as high as 1 μm/ns where two domains get connected. In general, domain-wall speeds extracted for domains that do not connect are much lower, and the propagation within 3 ns is comparable to the lateral resolution.

This result can be understood considering three energy contributions to E_{prop}: The Zeeman energy $-H_{\mathrm{ext}}M_S t$ of the film in the external field, the local interlayer coupling energy E_{copl}, and the change in domain-wall energy ΔE_{DW} upon expansion of existing domains. This is schematically explained in Fig. 3. Expansion of a rectangular domain of width w and length L along the magnetization axis by the darker areas increases the length of the vertical domain walls towards the top and bottom of the image, as indicated by the small thick lines. This corresponds to an increase in domain-wall energy per unit area of reversed domain surface of $\Delta E_{\mathrm{DW}}=2\gamma t/w$. Here, γ denotes the specific domain-wall energy per (cross-sectional) unit area. For the film thickness t considered here, domain walls are of the Néel type.[9] In this case, the domain-wall energy can be approximated by $\gamma=\sqrt{AM_S^2/(2\mu_0)}$. Using $A=13\times10^{-12}$ J/m for the exchange constant of permalloy, and $M_S=1.0$ T, one obtains $\gamma=2.3$ mJ/m^2. For $w=3$ μm, $\Delta E_{\mathrm{DW}}\approx 7.7$ μJ/m^2, which is smaller than the Zeeman energy of -18 μJ/m^2, but higher than the interlayer coupling energy of 1.6 μJ/m^2. For parallel domain walls separated by less than about $1000\sqrt{2\mu_0 A/M_S^2}\approx 5.7$ μm, the domain-wall energy γ may be additionally modified by up to 40% by the magnetostatic interaction between Néel walls.[9]

Figure 3(b) shows the case when the same domain is expanded along its width. In this case, the head-on charged domain walls at the top and bottom have to get longer. Because of the additional magnetostatic interaction between the domains, these walls have a higher specific energy $\gamma^\star>\gamma$. The change in domain-wall energy per unit area of reversed domain in this case is $\Delta E_{\mathrm{DW}}=2\gamma^\star t/L$.

The energy penalty ΔE_{DW} may be significantly reduced or may even reverse sign if two existing domains merge together. Such a case is schematically depicted in Fig. 3(c), where the pointed ends of two domains merge upon application of an external field. In this case, the (partly charged) domain walls indicated by thick dotted tilted lines disappear and are replaced by (uncharged) vertical domain-wall sections plotted by thick continuous lines. ΔE_{DW} is now the difference in energy between the dotted and continuous wall sections, and may be zero or even negative, depending on the actual geometry. In the sample discussed in this letter, the influence of ΔE_{DW} over E_{prop}, and therefore on the speed of magnetization reversal, is significant and favors domain connection, as can be clearly seen in Fig. 2.

In general, ΔE_{DW} scales inversely with the size of the domains, such that it becomes more important when the magnetization reversal proceeds by nucleation and expansion of many small domains. It has been shown that for fast magnetization reversal, an increase in dH_{ext}/dt is accompanied by an increase in the number of nucleated and subsequently expanded reversed domains.[5,10] The influence of the domain-wall energy will consequently play a role exactly in cases in which high fields are applied for short times in order to achieve high reversal speeds, and hence become important for the fast magnetization reversal of spin valve devices.

The authors thank F. Helbig, F. Senf, and G. Meyer for technical support, R. Hertel for valuable discussions, and F. Petroff and A. Vaurès for sample preparation. Financial support by BMBF (No. 05KS1 EFA6) and EU (BESSY-EU-HPRI 1999-CT-00028) is gratefully acknowledged.

[1] S. A. Wolf, D. D. Awschalom, R. A. Buhrman, J. M. Daughton, S. von Molnar, M. L. Roukes, A. Y. Chtchelkanova, and D. M. Treger, Science **294**, 1488 (2001).
[2] J. Stöhr, Y. Wu, B. D. Hermsmeier, M. G. Samant, G. R. Harp, S. Koranda, D. Dunham, and B. P. Tonner, Science **259**, 658 (1993).
[3] C. Won, Y. Z. Wu, A. Scholl, A. Doran, N. Kurahashi, H. W. Zhao, and Z. Q. Qiu, Phys. Rev. Lett. **91**, 147202 (2003).
[4] W. Kuch, L. I. Chelaru, F. Offi, J. Wang, M. Kotsugi, and J. Kirschner, Phys. Rev. Lett. **92**, 017201 (2004).
[5] J. Vogel, W. Kuch, M. Bonfim, J. Camarero, Y. Pennec, F. Offi, K. Fukumoto, J. Kirschner, A. Fontaine, and S. Pizzini, Appl. Phys. Lett. **82**, 2299 (2003).
[6] A. Krasyuk, A. Oelsner, S. A. Nepijko, A. Kuksov, C. M. Schneider, and G. Schönhense, Appl. Phys. A: Mater. Sci. Process. **76**, 863 (2003).
[7] J. Vogel, W. Kuch, J. Camarero, K. Fukumoto, Y. Pennec, M. Bonfim, S. Pizzini, F. Petroff, A. Fontaine, and J. Kirschner, J. Appl. Phys. **95**, 6533 (2004).
[8] W. Kuch, L. I. Chelaru, F. Offi, M. Kotsugi, and J. Kirschner, J. Vac. Sci. Technol. B **20**, 2543 (2002).
[9] A. Hubert and R. Schäfer, *Magnetic Domains* (Springer, Berlin, 1998).
[10] Y. Pennec, J. Camarero, J. C. Toussaint, S. Pizzini, M. Bonfim, F. Petroff, W. Kuch, F. Offi, K. Fukumoto, F. Nguyen Van Dau, and J. Vogel, Phys. Rev. B **69**, 180402 (2004).